Title

Spontaneous osteonecrosis of the jaws in the maxilla of mice on antiresorptive treatment: A novel ONJ mouse model

Authors

de Molon, Rafael Scaf
Cheong, Simon
Bezouglaia, Olga
et al.

Publication Date

2014-11-01

DOI

10.1016/j.bone.2014.07.027

Peer reviewed

HHS Public Access

Author manuscript

Bone. Author manuscript; available in PMC 2015 November 01.

Published in final edited form as:

Bone. 2014 November ; 68: 11–19. doi:10.1016/j.bone.2014.07.027.

Spontaneous Osteonecrosis of the Jaws in the Maxilla of Mice on Antiresorptive Treatment: A Novel ONJ Mouse Model

Rafael Scaf de Molon[1,2,*], **Simon Cheong**[3,*], **Olga Bezouglaia**[1], **Sarah M Dry**[4], **Flavia Pirih**[5], **Joni Augusto Cirelli**[2], **Tara L Aghaloo**[1,#], and **Sotirios Tetradis**[1,6,#]

[1]Division of Diagnostic and Surgical Sciences, UCLA School of Dentistry, Los Angeles, CA, 90095

[2]Department of Diagnosis and Surgery, School of Dentistry at Araraquara, São Paulo State University, Araraquara, 14801-903, Brazil

[3]Ostrow School of Dentistry, University of Southern California

[4]Department of Pathology and Laboratory Medicine, David Geffen School of Medicine at UCLA, Los Angeles, CA, 90095

[5]Division of Associated Specialties, UCLA School of Dentistry, Los Angeles, CA, 90095

[6]Molecular Biology Institute, UCLA, Los Angeles, CA, 90095

Abstract

Although osteonecrosis of the jaws (ONJ), a serious complication of antiresorptive medications, was reported a decade ago, the exact mechanisms of disease pathophysiology remain elusive. ONJ-like lesions can be induced in animals after antiresorptive treatment and experimental interventions such as tooth extraction or periapical or periodontal disease. However, experimental induction and manipulation of disease progression does not always reflect clinical reality. Interestingly, naturally occurring maxillofacial abscesses, inducing aggressive inflammation of the peri-radicular mucosa with significant osteolysis and alveolar bone expansion, have been reported in mice. Here, we aimed to explore whether osteonecrotic lesions would develop in areas of maxillary peri-radicular infections, in mice on antiresorptive medications with distinct pharmacologic action, thus establishing a novel ONJ animal model. Mice were treated with

[#]Corresponding Authors: Sotirios Tetradis, DDS, PhD, Diagnostic and Surgical Sciences, UCLA School of Dentistry, 10833 Le Conte Ave. CHS Rm. 53-068, Los Angeles, CA 90095-1668, Tel: (310) 825-5712, Fax: (310) 825-7232, stetradis@dentistry.ucla.edu. Tara L. Aghaloo, DDS, MD, PhD, Diagnostic and Surgical Sciences, UCLA School of Dentistry, 10833 Le Conte Ave. CHS Rm. 53-009, Los Angeles, CA 90095-1668, Tel: (310)794-7070, Fax: (310)825-7232, taghaloo@dentistry.ucla.edu.

[*]These authors contributed equally to this work

Authors' roles: All authors participated in the design, execution and analyses of the studies. TA, RSM, SC, and ST drafted the manuscript. All authors made revisions to the manuscript and approved the final version.

DISCLOSURES

Dr. Tetradis has served as a paid consultant for and has received grant support from Amgen Inc. All other authors state that they do not have any conflicts of interest.

RANK-Fc or OPG-Fc that bind to RANKL or with the potent bisphosphonate zoledronic acid (ZA). Maxillae were assessed radiographically and histologically. μCT imaging of vehicle mice revealed several maxillae with altered alveolar bone morphology, significant ridge expansion and large lytic areas. However, in RANK-Fc, OPG-Fc and ZA treated animals the extent of bone loss was significantly less, but exuberant bone deposition was noted at the ridge periphery. BV and BV/TV were increased in the diseased site of antiresorptive vs. veh animals. Histologically, extensive inflammation, bone resorption and marginal gingival epithelium migration were seen in the diseased site of vehicle animals. Rank-Fc, OPG-Fc and ZA reduced alveolar bone loss, increased periosteal bone formation, and induced areas of osteonecrosis, and bone exposure that in many animals covered significant part of the alveolar bone. Collectively, our data demonstrate ONJ-like lesions at sites of maxillary peri-radicular infection, indistinguishable in mice treated with RAKL inhibitors vs. zoledronate. This novel mouse model of spontaneous ONJ supports a central role of osteoclast inhibition and infection/inflammation in ONJ pathogenesis and validates and complements existing animal models employing experimental interventions.

Keywords

osteonecrosis of the jaw; ONJ; antiresorptives; bisphosphonates; alveolar bone; osteoclasts

1. INTRODUCTION

Osteonecrosis of the jaws (ONJ) is a serious side effect of antiresorptive medications such as bisphosphonates (BPs) and denosumab that ranges in severity from painless, small areas of exposed bone to significant bone exposure associated with severe pain, sequestration, infection, fistula or jaw fracture [1–3]. Although many clinical and animal studies attempt to characterize features of ONJ, the pathogenetic mechanisms of the disease remain elusive [4–6].

Osteoclastic inhibition appears central in the disease process since agents that target osteoclast function, but with distinct pharmacologic properties result in the same clinical outcome [1, 4–7]. Bisphosphonates and particularly nitrogen-containing ones, such as zoledronic acid (ZA), pamidronate, and alendronate, inhibit farnesyl diphosphate synthase in the cholesterol biosynthesis pathyway, which prevents prenylation of small guanosine triphosphatase (GTPase) signaling proteins [8, 9]. As a result, BPs inhibit functioning osteoclasts by impairing differentiation, disrupting the cytoskeleton, decreasing intracellular transport, and inducing apoptosis [9, 10]. In contrast, Denosumab binds directly to the receptor activator of nuclear factor kappa-B (RANK) ligand (RANKL) to prevent its interaction with RANK on osteoclasts. This binding inhibits osteoclast formation, differentiation, and function [11]. Although acting through diverse mechanisms, both BPs and denosumab show similar prevalence of ONJ in patients with multiple myeloma, breast, and prostate cancer [12–14].

ONJ occurs mostly after tooth extraction or around teeth with dental disease [15, 16]. Teeth in adult patients are extracted mainly as a result of unrestorable caries or periodontal disease [17, 18]. Thus, infection/inflammation due to dental disease appears to be present in most ONJ cases. Paralleling these clinical observations, animal findings demonstrate ONJ-like

lesions after experimental interventions such as tooth extraction or periapical or periodontal disease [19–30]. These interventions are employed to simulate clinical scenaria that precipitate disease pathogenesis in a controlled and reproducible manner.

Interestingly, naturally occurring maxillofacial abscesses have been described in mice [31]. Hair impaction from grooming enters the oral cavity, and inserts into the gingival sulcus where bacterial colonization occurs [31–33]. This natural process leads to the development of reproducible bone disease in C57BL/6 mice, which serves as an interesting contrast to the experimentally induced dental disease studies in mice and rats [19, 20, 23].

Here capitalizing on the natural occurrence of alveolar lesions, we aimed to explore the radiographic and histologic changes in the maxillae of mice treated with agents possessing distinct pharmacologic inhibition of osteoclastic activity. Our data suggest that in this novel ONJ animal model, naturally occurring peri-radicular infection and antiresorptive treatment are sufficient to induce osteonecrotic lesions in the mouse maxilla.

2. MATERIALS AND METHODS

2.1 Animal Care

Animals were kept and treated according to guidelines of the UCLA Chancellor's Animal Research Committee. Throughout the experimental period, mice were housed in plastic cages, fed a standard laboratory diet, and given water ad libitum. Seventy-six 4-month old C57BL/6J male mice (Jackson Laboratories, Bar Harbor, ME, USA) received intraperitoneal (IP) injections of veh (endotoxin free saline) or 200 μg/kg zoledronic acid (ZA, Z-5744 LKT laboratories, St. Paul, MN) three times per week or 10 mg/kg mouse RANK-Fc (composed of the extracellular domain of RANK fused to the Fc portion of IgG [34], kindly provided by Amgen, Inc, Thousand Oaks, CA) three times per week, or 10 mg/kg rat OPG-Fc (composed of the RANKL-binding domains of osteoprotegerin linked to the Fc portion of IgG [34, 35], kindly provided by Amgen, Inc, Thousand Oaks, CA) once per week for a total of 12 weeks. The time and dose of these antiresorptives have been previously shown to induce ONJ-like lesions in mice with periapical disease [19, 23]. There were 17 veh, 19 ZA, 20 OPG-Fc and 20 RANK-Fc treated animals. At the end of the experiment, animals were sacrificed via isoflurane overdose, and maxillae were dissected, placed in 4% paraformaldehyde for 48 hours and stored in 70% ethanol.

2.2 μCT Scanning

Dissected maxillae were imaged by μCT scanning (μCT SkyScan 1172; SkyScan, Kontich, Belgium) utilizing 57 kVp, 184 μA, 0.5 mm aluminum filtration and 10 μm resolution. For linear measurements, volumetric image data were converted to DICOM format and imported in the Dolphin Imaging software (Chatsworth, CA) to generate 3D and multiplanar reconstructed images. The periodontal ligament (PDL) space width was measured at the furcation area of the first molar. The cemento-enamel junction (CEJ) to the alveolar crest (AC) distance was measured at the distal surface of the first molar. Both measurements were performed on a sagittal slice through the middle of the furcation area along the mesio-distal axis of the teeth, as previously described [19]. To assess alveolar bone thickness, axial slices

were oriented parallel to the occlusal plane and the bone width was measured at the buccal side of the alveolar ridge at the level of the apical third of the roots.

To measure alveolar bone volume (BV) and tissue volume (TV), a region of interest (ROI) was delineated from the mesial root of the first molar to the distal root of the third molar, and from the alveolar crest to the root apices, comprising the entire alveolar bone. The teeth roots were not included in the ROI. BV and TV were measured utilizing the CtAn software (CT Analyzer 1.10.1.0 - Skyscan, Kontich, Belgium).

2.3 Histology and TRAP staining

Maxillae were decalcified in 14.5% ethylenediaminetetraacetic acid (EDTA) solution for three weeks. Samples were paraffin embedded and 5 μm-thick cross sections were made perpendicular to the long axis of the alveolar ridge at the area of maximum radiographic changes, as assessed by μCT analysis. If no radiographic evidence of disease was present in either of the sides of the alveolar bone, then sections were made along the distal root of the first molar. Hematoxylin and eosin (H&E) stained slides were digitally scanned utilizing the Aperio AT automated slide scanner and the Aperio ImageScope software (Aperio Technologies, Inc., Vista, CA, USA). The area of the alveolar bone, from the alveolar crest to the superior border of the alveolar bone and the floor of the nasal cavity was defined as the region of interest (ROI). All subsequent measurements were made in this area.

Histologic measurements were made as previously described [19]. The distance between the most apical point of the junctional epithelium to the most coronal point of the alveolar crest (JE-AC) was measured on the palatal side of the maxilla. Periosteal bone thickness was assessed by measuring the three greatest areas of palatal or buccal periosteal thickness that were then averaged. The total number of osteocytic lacunae, the number of empty lacunae, the surface of total bone area and the surface of osteonecrotic area(s) were quantified. An area of osteonecrosis was defined as a loss of more than five contiguous osteocytes with confluent areas of empty lacunae. All histology and digital imaging was performed at the Translational Pathology Core Laboratory (TPCL) at UCLA.

For enumeration of osteoclasts, tartrate-resistant acid phosphatase (TRAP) staining was performed from all the groups utilizing the leukocyte acid phosphatase kit (387A-IKT Sigma Aldrich, St. Louis, MO, USA). Positive cells were identified as multinucleated (≥3) TRAP-positive cells in contact with or very close proximity to the bone surface, in the ROI.

2.4 Statistics

Raw data were analyzed using the GraphPad Prism Software (GraphPad Software, Inc. La Jolla, CA). Descriptive statistics were used to calculate the mean and the standard error of the mean (SEM). Data among groups were analyzed using one-way analysis of variance (ANOVA) followed by the post-hoc Tukey's test for multiple comparisons. Data between groups (healthy vs. diseased) were compared using the Student's t test. Categorical data (Table 1) were analyzed using the Fisher's exact test.

3. RESULTS

μCT imaging of the maxillae revealed many animals with normal alveolar bone architecture, reflected by a uniform periodontal ligament (PDL) space (Fig 1, thin arrow) and a continuous thin lamina dura around the roots of the teeth in all treatment groups. However, several veh treated mice presented altered alveolar bone morphology. Large lytic areas were noted around the roots and the furcational area of the maxillary molars that in select animals extended almost to the root apex and surrounded the entire root (Fig 1, arrow). Additionally, significant superior, buccal and palatal expansion of the alveolar ridge was observed (Fig 1, arrowheads). Several RANK-Fc, OPG-Fc and ZA treated animals showed similar lytic lesions to the veh group, although the extent of bone loss was significantly less (Fig 1, arrows). Substantial periosteal bone apposition was noted at the periphery of the alveolar ridge that resulted in marked bone expansion (Fig 1, arrowheads). The radiographic appearance of the alveolar bone was indistinguishable among the RANK-Fc, OPG-Fc or ZA groups.

To quantify the amount of bone loss in the diseased sites, the distance from the cemento-enamel junction (CEJ) to the alveolar crest (AC) at the distal surface of the 1st molar was measured. An increased CEJ-AC distance denotes increased bone loss. Diseased vs. healthy sites demonstrated statistically significantly increased CEJ-AC distance for all treatment groups (Fig 2A). Importantly, statistically significantly larger CEJ-AC distance was seen in the diseased site of veh group compared to the same site in the RANK-Fc, OPG-Fc and ZA groups (Fig 2A). No difference among the three antiresorptive treated groups was detected.

To evaluate effects on PDL space, the PDL space width was assessed at the furcation of the first maxillary molars [19, 20, 23]. No differences were seen among the healthy sites in any of the treatment groups. For all groups, a statistically significant widening of the PDL space was observed in the diseased vs. healthy sites (Fig. 2B). Diseased sites in veh treated animals showed a significantly higher increase in PDL space width compared to the antiresorptive treatment groups (Fig 2B).

To quantify the alveolar bone expansion, the buccal bone thickness at the level of the apical third of the roots was measured (Fig 2C). A significant expansion of the alveolar bone was seen at the diseased vs. healthy site in all groups. However, a statistically significantly greater increase was present in the RANK-Fc, OPG-Fc and ZA vs. veh groups, while no difference was detected among antiresorptive treated animals (Fig 2C).

To evaluate the overall effects of the maxillary infection and antiresorptive treatment in the bone architecture, BV, TV and BV/TV of the alveolar ridge were measured (Fig 2D, E, F). No difference was seen between the healthy vs. diseased sites in veh animals. Healthy alveolar bone in RANK-Fc, OPG-Fc and ZA showed a similar increase in BV vs. the veh group. Diseased sites in the antiresorptive treated mice showed an even further increase in BV, compared to the healthy site of the same animals or the healthy or diseased site of the veh group (Fig 2, D). TV was similarly increased in the diseased site of all groups (Fig 2E), reflecting the observed alveolar bone expansion. BV/TV was significantly decreased in the diseased site of veh group compared to the healthy site of the same animals, but also

compared to the healthy or diseased site of all antiresorptive treatment groups (Fig 2F). As expected, antiresorptive vs. veh animals showed increased BV/TV in the healthy sites (Fig 2F). Finally, a small but statistically significant decrease in BV/TV was noted for the diseased vs. healthy site in each of the RANK-Fc, OPG-Fc and ZA groups (Fig 2F).

After μCT assessment, histologic evaluation of the maxillae was performed (Fig 3). Healthy sites in all groups showed normal alveolar bone and marginal epithelium (Fig 3, A, B, C, D, turquoise and red arrows). In vehicle treated animals, an abundant inflammatory infiltrate (Fig 3E, E′, black arrows) composed of acute (neutrophils) and chronic (lymphocytes) inflammatory cells was noted. Inflammation was present in both the epithelium and underlying mucosa. Migration of the marginal epithelium (Fig 3E, E′, red arrows) was paralleled by marked bone loss (Fig 3E, E′, turquoise arrows) such that the marginal epithelium distance appeared increased. No histologic evidence of osteonecrosis was seen in any of the samples. However, new bone formation at the alveolar bone perimeter (Fig 3E, E ′, blue arrows) was present.

Comparable histologic features were present at the diseased site among animals treated with all three antiresorptive treatments - RANK-Fc (Fig 3F, F′), OPG-Fc (Fig 3G, G′) and ZA (Fig 3H, H′). Similar to the veh treated animals, abundant mixed (acute and chronic) inflammatory infiltrate was noted in both the epithelium and soft tissue (Fig 3F, F′, G, G′, H, H′, black arrows). Bone loss was present compared to healthy sites, but appeared less compared to the diseased site of the veh treated mice (Fig 3F, F′, G, G′, H, H′, turquoise arrows). However, marked marginal epithelium migration was noted (Fig 3F, F′, G, G′, H, H ′, red arrows), such that the epithelium to alveolar crest distance was reduced. Areas of osteonecrosis, with empty osteocytic lacunae, were present in many specimens from the diseased site of all antiresorptive treated animals (Fig 3F, F′, G, G′, H, H′, yellow arrows). In several specimens, the necrotic bone was not covered by oral mucosa, but was exposed to the oral cavity (Fig 3F, F′, G′, green arrows).

Three main patterns of histologic appearance were noted in the diseased site of antiresorptive treated animals (Fig 4) that were indistinguishable among the antiresorptive treatment groups (RANK-Fc (Fig 4A, B, C), OPG-Fc (Fig 4D, E, F) or ZA (Fig 4G, H, I). First, abundant inflammation and periosteal bone formation were present (Fig 4A, D, G, black and blue arrows). However, no areas of osteonecrosis were detected. Second, in addition to the inflammatory bone changes, specimens showed areas of osteonecrosis with empty osteocytic lacunae (Fig 4B, E, H, black, blue and yellow arrows). Epithelial migration towards the osteonecrotic areas was noted, however, no bone exposure was observed (Fig 4B). The third pattern, in addition to inflammation and osteonecrosis, presented with bone exposure (Fig 4C, F, I, black, yellow and green arrows). Significant epithelial migration along the surface of the necrotic bone to the level of vital bone resulted in significant exposure of the osteonecrotic areas to the oral cavity (Fig 4C, F, I, red arrows) that included the palatal alveolar ridge and extended nearly to the midline.

Table 1 summarizes the radiographic and histologic observations of these studies. The incidence of peri-radicular disease in the various treatment groups ranged from 39.4–58% with no statistical significant differences detected among the various groups. The diseased

site of all animals showed alveolar bone expansion, irrelevant of the treatment. Osteonecrosis and bone exposure were only observed in animals on antiriesorptives. Interestingly, only 45–71% of the diseased hemimaxillae showed areas of osteonecrosis. However, from the sites with osteonecrosis, 70–80% presented with bone exposure. No difference on the incidence of osteonecrosis or bone exposure was detected among RANK-Fc, OPG-Fc or ZA treated groups.

We then quantified histologic findings and performed comparisons among treatment groups. A significant increase of the JE-AC distance was noted for the diseased site of the veh treated group, probably reflecting the significant periradicular bone loss (Fig 5A). In contrast, antiresorptive treatment reversed the effect on the JE-AC distance that was shorter in the diseased vs. healthy sites for RANK-Fc, OPG-Fc and ZA treated groups, likely as a result of junctional epithelium migration, but reduced bone resorption (Fig 5A). Periosteal thickness significantly increased in the diseased vs. healthy site for all groups. However, this increase was greater for the RANK-Fc, OPG-Fc or ZA vs. veh treated animals (Fig 5B).

To evaluate the effect of antiresorptives on osteocytes and induction of osteonecrosis, the number of empty osteocytic lacunae (Fig 5C) and the osteonecrotic surface area (Fig 5D) were evaluated at the area of the maxillary alveolar ridge. No empty osteocytic lacunae or areas of osteonecrosis were detected in the healthy or diseased sites of the veh treated mice. Healthy sites of RANK-Fc, OPG-Fc and ZA treated animals showed a slight increase in the number of empty osteocytic lacunae that did not reach statistical significance (Fig 5C). In contrast, significant increase of empty osteocytic lacunae (Fig 5C) and areas of osteonecrosis (Fig 5D) were present in the diseased site of RANK-Fc, OPG-Fc or ZA treated mice. A small but significantly higher number of empty osteocytic lacunae was seen in the diseased site of OPG-Fc vs. ZA treated mice (Fig 5C). However, no difference in osteonecrotic areas was noted among the three antiresorptive treatments (Fig 5D). The osteonecrotic areas covered 16.9 %, 22.9 %, and 16.0 % of the ROI and measured 135,479 +/− 31,403, 180,368 +/− 25,106, and 139,440 +/− 39,923 μm^2 for RANK-Fc, OPG-Fc and ZA groups, respectively.

To evaluate the effect of the antiresorptive treatments on osteoclast numbers, TRAP staining was performed (Fig 6). Few TRAP+ cells were observed at the healthy site (Fig 6A) and were significantly increased at the diseased site (Fig 6E) of the veh treated animals. As expected, RANK-Fc and OPG-Fc treatment nearly abolished osteoclast formation in both healthy and diseased sites (Fig 6.B, C, F, G) Interestingly, TRAP+ cells that significantly increased in the diseased site were noted in ZA treated animals (Fig 6D, H). However, TRAP+ cells in ZA treated animals showed a round shape with pyknotic nuclear morphology and were detached and at times moved from the bone surface (Fig 6I). Quantification of TRAP staining revealed significant inhibition of osteoclast formation by RANK-Fc and OPG-Fc treatment compared to control and ZA groups (Fig 6J). No statistical difference of the TRAP+ cell number between the diseased site of veh vs. ZA treated mice was found (Fig 6I).

4. DISCUSSION

ONJ occurs mainly after tooth extraction in patients treated with medications that target osteoclastic function and activity, such as BPs and Denosumab, for the treatment of neoplastic or metabolic bone disease [2, 36]. Several animal models have utilized tooth extraction and high-dose BPs to reproduce clinical, radiographic and histologic features of the human disease [21, 24, 37].

Since the great majority of tooth extractions in adults is due to advanced carious lesions or periodontal bone loss [17, 18], and given that dental preventive measures reduce the risk for ONJ [38, 39] and that a significant number of ONJ cases occurs in the absence of tooth extraction, we have hypothesized that dental disease plays a key role in ONJ pathogenesis [19, 20, 23]. Indeed, we and others have presented rat and mouse ONJ models in the absence of tooth extraction but in the presence of aggressive periodontitis or periapical disease in animals treated with high dose BPs [20, 22, 23, 26] or RANKL inhibitors [19] thus pointing to a central role of infection/inflammation in ONJ pathophysiology [4–6].

For these ONJ animal models, established models of experimental dental disease were employed. Advantage of such approaches are the well characterized progression of dental disease, the localization of dental disease in a split-mouth design providing internal controls, and the control of onset of dental disease in relation to administration of antiresorptive medication. However, experimental induction and manipulation of disease progression does not always reflect clinical reality. To that effect, several ONJ animal models utilize extraction of healthy teeth [21, 24, 25, 27–30], which are rarely extracted in ONJ patients. Similarly, ONJ animal models utilizing periodontitis [20, 22, 26] employ experimental procedures that depict some, but not necessarily all the components of the pathological process of human periodontal disease [40]. Finally, in ONJ models of antiresorptives and periapical disease drilling the crown of molars to induce pulpal exposure [22, 26], although captures the pathophysiologic progression of pulp necrosis and periapical infection does not reflect the natural pulpal infection through deep carious lesions.

Naturally occurring maxillofacial abscesses have been reported in mice, including the inbred C57BL/6 strain [31–33]. The mice develop these abscesses from barbering practices including grooming, plucking, or eating fur or whiskers of cage-mates or oneself [41–43]. C57BL/6 mice are one of the most common rodent strains where barbering, mastication, and fragmentation of hair, occurs [41, 43]. Here, the foreign body gets into the oral cavity, pierces the gingival sulcus, and induces dental disease [31]. After hair impaction, bacterial colonization occurs, and cultures consistently reveal staphylococcus aureus isolated from the abscesses [31–33]. μCT of these areas demonstrate osteolysis with severe bone loss surrounding the molar roots and expansion of the alveolar bone [31]. Histologically, severe inflammatory infiltrate with presence of neutrophils and mononuclear inflammatory cells is reported [31, 32]. Intrigued by this spontaneous occurrence of peri-radicular infection and resultant extensive inflammation, we investigated the potential development of ONJ-like lesions in the maxillae of mice that had been treated with high-dose antiresorptive medications, thus establishing a novel ONJ animal model. An advantage of this model is the

natural occurrence or peri-radicular infection/inflammation, without the need of experimental interventions.

We utilized two classes of antiresorptive agents with distinct pharmacologic actions. RANK-Fc and OPG-Fc bind and inhibit RANKL function and were used as a surrogate for Denosumab, since Denosumab recognizes the human but not mouse RANKL [34]. Both RANK-Fc and OPG-Fc bind RANKL and potently inhibit bone resorption and increase bone volume in animal models [34, 35]. The second type of antiresorptive was zoledronic acid (ZA), a potent nitrogen-containing bisphosphonate widely used in the management of bone malignancy [44]. Utilizing the employed treatment regimens for these antiresorptives, we have previously reported the successful inhibition of osteoclastic function and development of ONJ-like lesions in the mandible of mice around mandibular molars with experimental periapical disease [19, 23].

Similar to published data [31, 32], μCT assessment of the alveolar bone revealed significant peri-radicular osteolysis and expansion of the buccal and palatal cortices of the alveolar ridge in several veh treated mice. Antiresorptives attenuated interproximal and furcational bone loss at and increased overall alveolar bone volume at the diseased sites. These observations are in agreement with findings around experimental periodontal or periapical disease in rats or mice [19, 20, 23] and parallel clinical findings that demonstrate diffuse osteosclerosis with increased trabecular density and thickening of cortical outlines in areas of ONJ [45].

Histologically, the presence of intense inflammation, significant osteolysis and epithelial migration was seen in the periodontal tissues of several control (veh treated) mice, similar to previous reports [31, 32]. Presence of inflammation was also noted on antiresorptive-treated groups. However, loss of osteocytes and presence of empty osteocytic lacunae consistent with osteonecrosis were also present in these animals. Presence of osteonecrosis has been described in animals on antiresorptives after tooth extraction or experimental disease, emphasizing the resemblance of the spontaneous ONJ-like lesions observed in our studies with other ONJ-animal models [19–30]. The similar radiographic and histologic disease presentation between this and other ONJ models [19–30], which parallels findings in ONJ patients validates such animal models as capturing essential features of disease pathophysiology that lead to alveolar bone osteonecrosis.

A noteworthy observation in our studies was the great similarity in the radiographic and histologic findings among the RANK-Fc, OPG-Fc and ZA treated groups, including the incidence of osteonecrosis and bone exposure. Indeed, to the best of our knowledge, this is the second report of antiresorptive treatment, other than bisphosphonates, inducing ONJ-like lesions in an animal model [19] and the first direct comparison of these different antiresorptive categories. Our findings parallel human data from BP vs. Denosumab treated patients reporting a similar incidence of ONJ [12–14] and strongly point to a central role of osteoclastic inhibition in ONJ pathogenesis.

Utilizing this ONJ mouse model, we observed three histologic patterns at sites of disease that were similar for all three antiresorptives (Fig 4 and Table 1). In the first pattern,

significant inflammation throughout the alveolar ridge and varying amount of osteolysis were noted. However, similar to the veh treated group, no osteonecrosis was present. In the clinical setting, these animals could potentially parallel patients on antiresorptive medications and jaw inflammation but without any clinical or radiographic signs of ONJ. In the second pattern, osteonecrotic areas were present within the alveolar bone but were covered by oral mucosa. This disease appearance appears to parallel Stage 0 ONJ in patients with bone necrosis, but without clinical bone exposure [2]. Finally, in the third pattern the necrotic alveolar bone was not covered by oral mucosa but was exposed to the oral environment. This presentation is in line with the classic manifestation of clinical ONJ with varying degree of bone exposure and associated infection/inflammation (Stage 1–3 ONJ) [2]. Our present studies cannot address whether a transition from less towards higher stage ONJ exists, since we only examined the animals at a single time point. However, clinical data reporting 50% of patients with stage 0 disease developing clinical ONJ within five months of initial diagnosis [46], would argue for the progression of the less severe histologic osteonecrosis without bone exposure to the more severe presentation of bone necrosis and clinical exposure.

A surprising and interesting finding was the difference on osteonecrosis incidence in this ONJ mouse model with spontaneous maxillary infection vs. studies utilizing experimental periapical disease [19, 23], although treatment regimens for various antiresorptives were the same. In the current study, approximately 50% of the animals with peri-radicular disease presented with areas of osteonecrosis. In contrast, 88% of ZA [23] or 100% of RANK-Fc or OPG-Fc [19] treated mice with experimental periapical disease showed osteonecrotic areas histologically.

A possible explanation for this finding is that maxilla (in the current study) vs. mandible [19, 23] respond different to bone turnover suppression. In contrast to osteoradionecrosis that almost exclusively localizes to the mandible [47], ONJ appears to affect both jaws with high frequency. However, even in the case of ONJ the mandible appears to be more frequently affected, particularly in patients treated with antiresorptives for the treatment of osteoporosis [2, 48, 49]. The predilection of the mandible for osteonecrosis could be due to the decreased vascularity, thicker cortical borders and smaller percentage of trabecular bone [50, 51].

A second possible explanation for this observation is the relation of antiresorptive administration with the disease onset. Maxillary lesions developed spontaneously without any intervention. Thus, some animals developed maxillary inflammatory lesions prior to, while others after the commencement of antiresorptives. In contrast, experimental periodontitis or periapical disease was induced after antiresorptive medications were administered [19, 20, 23, 26]. Possibly the early stages of infection and resultant inflammatory response could play a crucial role in the alveolar bone response to turnover suppression. Such a premise would be significant from a clinical perspective, since it points to the potential association between antiresorptive administration and time of peri-radicular infection.

Interesting, although osteonecrosis incidence was lower in the current ONJ model, bone exposure was more frequent and extensive compared to published studies [19, 20, 23]. Here,

nearly 75% of animals with osteonecrosis showed bone exposure that at times involved a significant part of the maxillary alveolar bone. In contrast, only 28% of animals with osteonecrosis presented bone exposure that was mostly localized to the marginal periodontium when experimental periapical disease was induced [19, 23]. The most likely explanation for these observations is the degree of infection and resultant inflammatory changes that in the current study extended to the whole alveolus and caused significant buccal and palatal bone deposition and marked ridge expansion.

Our findings have potentially significant implications for studies on ONJ animal models utilizing maxillary molar extraction, particularly if the C57BL6 strain of mice were used [21, 24]. Since in many of these studies animals were pretreated with bisphosphonates prior to tooth extraction, the possible presence of naturally occurring peri-radicular lesions in some sites could complicate socket healing and confound ONJ incidence and severity.

In conclusion, our data offer potentially important insights into the mechanisms of ONJ. The nearly identical radiographic and histologic features of alveolar bone morphology and ONJ-like appearance between the RANKL inhibitors OPG-Fc and RANK-Fc, and the potent bisphosphonate ZA parallel clinical findings and strongly indicate a central role of osteoclasts in ONJ pathophysiology. The reduced incidence of osteonecrosis compared to previously published reports suggests the significance of the onset of infection/inflammation in relation to the commencement of antiresorptive treatment, while the increased frequency and extent of alveolar bone exposure points to the link between the severity of inflammation and clinical ONJ severity. From a practical point of view, our observations caution the design and interpretation of experimental findings utilizing interventional approaches, as they might be compounded by the occurrence of spontaneous ONJ lesions around naturally occurring maxillary lesions of animals treated with antiresorptives. Finally, this novel model of spontaneous ONJ validates, compliments and enhances published ONJ models that utilize tooth extraction or experimental induction of dental disease and strongly supports the central importance of infection/inflammation in combination with inhibition of osteoclastic function in ONJ pathogenesis.

Acknowledgments

This work was supported by grant support from Amgen Inc, and by NIH/NIDCR DE019465. de Molon RS was supported by fellowships from the State of Sao Paulo Research Foundation #2012/09968-5 and the Coordination for the Improvement of Higher Level -or Education- Personnel - #11575/13-1.

References

1. Lipton A, Fizazi K, Stopeck AT, Henry DH, Brown JE, Yardley DA, Richardson GE, Siena S, Maroto P, Clemens M, Bilynskyy B, Charu V, Beuzeboc P, Rader M, Viniegra M, Saad F, Ke C, Braun A, Jun S. Superiority of denosumab to zoledronic acid for prevention of skeletal-related events: a combined analysis of 3 pivotal, randomised, phase 3 trials. Eur J Cancer. 2012; 48:3082–92. [PubMed: 22975218]
2. Ruggiero SL, Dodson TB, Assael LA, Landesberg R, Marx RE, Mehrotra B. American Association of O Maxillofacial S. American Association of Oral and Maxillofacial Surgeons position paper on bisphosphonate-related osteonecrosis of the jaws--2009 update. J Oral Maxillofac Surg. 2009; 67:2–12. [PubMed: 19371809]

3. Khosla S, Burr D, Cauley J, Dempster DW, Ebeling PR, Felsenberg D, Gagel RF, Gilsanz V, Guise T, Koka S, McCauley LK, McGowan J, McKee MD, Mohla S, Pendrys DG, Raisz LG, Ruggiero SL, Shafer DM, Shum L, Silverman SL, Van Poznak CH, Watts N, Woo SB, Shane E. American Society for B Mineral R. Bisphosphonate-associated osteonecrosis of the jaw: report of a task force of the American Society for Bone and Mineral Research. J Bone Miner Res. 2007; 22:1479–91. [PubMed: 17663640]
4. Allen MR, Burr DB. The pathogenesis of bisphosphonate-related osteonecrosis of the jaw: so many hypotheses, so few data. J Oral Maxillofac Surg. 2009; 67:61–70. [PubMed: 19371816]
5. Landesberg R, Woo V, Cremers S, Cozin M, Marolt D, Vunjak-Novakovic G, Kousteni S, Raghavan S. Potential pathophysiological mechanisms in osteonecrosis of the jaw. Ann N Y Acad Sci. 2011; 1218:62–79. [PubMed: 21291478]
6. Yamashita J, McCauley LK. Antiresorptives and osteonecrosis of the jaw. J Evid Based Dent Pract. 2012; 12:233–47. [PubMed: 23040351]
7. Aghaloo TL, Felsenfeld AL, Tetradis S. Osteonecrosis of the jaw in a patient on Denosumab. J Oral Maxillofac Surg. 2010; 68:959–63. [PubMed: 20149510]
8. Luckman SP, Hughes DE, Coxon FP, Graham R, Russell G, Rogers MJ. Nitrogen-containing bisphosphonates inhibit the mevalonate pathway and prevent post-translational prenylation of GTP-binding proteins, including Ras. J Bone Miner Res. 1998; 13:581–9. [PubMed: 9556058]
9. Kimmel DB. Mechanism of action, pharmacokinetic and pharmacodynamic profile, and clinical applications of nitrogen-containing bisphosphonates. J Dent Res. 2007; 86:1022–33. [PubMed: 17959891]
10. Suzuki K, Takeyama S, Sakai Y, Yamada S, Shinoda H. Current topics in pharmacological research on bone metabolism: inhibitory effects of bisphosphonates on the differentiation and activity of osteoclasts. J Pharmacol Sci. 2006; 100:189–94. [PubMed: 16518076]
11. Baron R, Ferrari S, Russell RG. Denosumab and bisphosphonates: different mechanisms of action and effects. Bone. 2011; 48:677–92. [PubMed: 21145999]
12. Dranitsaris G, Hatzimichael E. Interpreting results from oncology clinical trials: a comparison of denosumab to zoledronic acid for the prevention of skeletal-related events in cancer patients. Support Care Cancer. 2012; 20:1353–60. [PubMed: 22539050]
13. Saad F, Brown JE, Van Poznak C, Ibrahim T, Stemmer SM, Stopeck AT, Diel IJ, Takahashi S, Shore N, Henry DH, Barrios CH, Facon T, Senecal F, Fizazi K, Zhou L, Daniels A, Carriere P, Dansey R. Incidence, risk factors, and outcomes of osteonecrosis of the jaw: integrated analysis from three blinded active-controlled phase III trials in cancer patients with bone metastases. Ann Oncol. 2012; 23:1341–7. [PubMed: 21986094]
14. Smith MR, Saad F, Coleman R, Shore N, Fizazi K, Tombal B, Miller K, Sieber P, Karsh L, Damiao R, Tammela TL, Egerdie B, Van Poppel H, Chin J, Morote J, Gomez-Veiga F, Borkowski T, Ye Z, Kupic A, Dansey R, Goessl C. Denosumab and bone-metastasis-free survival in men with castration-resistant prostate cancer: results of a phase 3, randomised, placebo-controlled trial. Lancet. 2012; 379:39–46. [PubMed: 22093187]
15. Ficarra G, Beninati F, Rubino I, Vannucchi A, Longo G, Tonelli P, Pini Prato G. Osteonecrosis of the jaws in periodontal patients with a history of bisphosphonates treatment. J Clin Periodontol. 2005; 32:1123–8. [PubMed: 16212571]
16. Marx RE, Sawatari Y, Fortin M, Broumand V. Bisphosphonate-induced exposed bone (osteonecrosis/osteopetrosis) of the jaws: risk factors, recognition, prevention, and treatment. J Oral Maxillofac Surg. 2005; 63:1567–75. [PubMed: 16243172]
17. Chrysanthakopoulos NA. Reasons for extraction of permanent teeth in Greece: a five-year follow-up study. Int Dent J. 2011; 61:19–24. [PubMed: 21382029]
18. Phipps KR, Stevens VJ. Relative contribution of caries and periodontal disease in adult tooth loss for an HMO dental population. J Public Health Dent. 1995; 55:250–2. [PubMed: 8551465]
19. Aghaloo TL, Cheong S, Bezouglaia O, Kostenuik P, Atti E, Dry SM, Pirih FQ, Tetradis S. RANK-L inhibitors induce osteonecrosis of the jaw in mice with periapical disease. J Bone Miner Res. 2013

20. Aghaloo TL, Kang B, Sung EC, Shoff M, Ronconi M, Gotcher JE, Bezouglaia O, Dry SM, Tetradis S. Periodontal disease and bisphosphonates induce osteonecrosis of the jaws in the rat. J Bone Miner Res. 2011; 26:1871–82. [PubMed: 21351151]
21. Bi Y, Gao Y, Ehirchiou D, Cao C, Kikuiri T, Le A, Shi S, Zhang L. Bisphosphonates cause osteonecrosis of the jaw-like disease in mice. Am J Pathol. 2010; 177:280–90. [PubMed: 20472893]
22. Gotcher JE, Jee WS. The progress of the periodontal syndrome in the rice cat. II. The effects of a diphosphonate on the periodontium. J Periodontal Res. 1981; 16:441–55. [PubMed: 6459441]
23. Kang B, Cheong S, Chaichanasakul T, Bezouglaia O, Atti E, Dry SM, Pirih FQ, Aghaloo TL, Tetradis S. Periapical disease and bisphosphonates induce osteonecrosis of the jaws in mice. J Bone Miner Res. 2013; 28:1631–40. [PubMed: 23426919]
24. Kikuiri T, Kim I, Yamaza T, Akiyama K, Zhang Q, Li Y, Chen C, Chen W, Wang S, Le AD, Shi S. Cell-based immunotherapy with mesenchymal stem cells cures bisphosphonate-related osteonecrosis of the jaw-like disease in mice. J Bone Miner Res. 2010; 25:1668–79. [PubMed: 20200952]
25. Sonis ST, Watkins BA, Lyng GD, Lerman MA, Anderson KC. Bony changes in the jaws of rats treated with zoledronic acid and dexamethasone before dental extractions mimic bisphosphonate-related osteonecrosis in cancer patients. Oral Oncol. 2009; 45:164–72. [PubMed: 18715819]
26. Aguirre JI, Akhter MP, Kimmel DB, Pingel JE, Williams A, Jorgensen M, Kesavalu L, Wronski TJ. Oncologic doses of zoledronic acid induce osteonecrosis of the jaw-like lesions in rice rats (Oryzomys palustris) with periodontitis. J Bone Miner Res. 2012; 27:2130–43. [PubMed: 22623376]
27. Lopez-Jornet P, Camacho-Alonso F, Martinez-Canovas A, Molina-Minano F, Gomez-Garcia F, Vicente-Ortega V. Perioperative antibiotic regimen in rats treated with pamidronate plus dexamethasone and subjected to dental extraction: a study of the changes in the jaws. J Oral Maxillofac Surg. 2011; 69:2488–93. [PubMed: 21798645]
28. Allen MR, Burr DB. Mandible matrix necrosis in beagle dogs after 3 years of daily oral bisphosphonate treatment. J Oral Maxillofac Surg. 2008; 66:987–94. [PubMed: 18423290]
29. Hokugo A, Christensen R, Chung EM, Sung EC, Felsenfeld AL, Sayre JW, Garrett N, Adams JS, Nishimura I. Increased prevalence of bisphosphonate-related osteonecrosis of the jaw with vitamin D deficiency in rats. J Bone Miner Res. 2010; 25:1337–49. [PubMed: 20200938]
30. Kuroshima S, Yamashita J. Chemotherapeutic and antiresorptive combination therapy suppressed lymphangiogenesis and induced osteonecrosis of the jaw-like lesions in mice. Bone. 2013; 56:101–9. [PubMed: 23727433]
31. Lawson GW. Etiopathogenesis of mandibulofacial and maxillofacial abscesses in mice. Comp Med. 2010; 60:200–4. [PubMed: 20579435]
32. Clarke MC, Taylor RJ, Hall GA, Jones PW. The occurrence in mice of facial and mandibular abscesses associated with Staphylococcus aureus. Lab Anim. 1978; 12:121–3. [PubMed: 152826]
33. Grant N, Jackson K, Lee R, Scharf B. Mandibular mass in a young Swiss-Webster mouse. Lab Anim (NY). 2002; 31:25–6. [PubMed: 12200582]
34. Kostenuik PJ, Nguyen HQ, McCabe J, Warmington KS, Kurahara C, Sun N, Chen C, Li L, Cattley RC, Van G, Scully S, Elliott R, Grisanti M, Morony S, Tan HL, Asuncion F, Li X, Ominsky MS, Stolina M, Dwyer D, Dougall WC, Hawkins N, Boyle WJ, Simonet WS, Sullivan JK. Denosumab, a fully human monoclonal antibody to RANKL, inhibits bone resorption and increases BMD in knock-in mice that express chimeric (murine/human) RANKL. J Bone Miner Res. 2009; 24:182–95. [PubMed: 19016581]
35. Lacey DL, Boyle WJ, Simonet WS, Kostenuik PJ, Dougall WC, Sullivan JK, San Martin J, Dansey R. Bench to bedside: elucidation of the OPG-RANK-RANKL pathway and the development of denosumab. Nat Rev Drug Discov. 2012; 11:401–19. [PubMed: 22543469]
36. Barasch A, Cunha-Cruz J, Curro FA, Hujoel P, Sung AH, Vena D, Voinea-Griffin AE, Group CC, Beadnell S, Craig RG, DeRouen T, Desaranayake A, Gilbert A, Gilbert GH, Goldberg K, Hauley R, Hashimoto M, Holmes J, Latzke B, Leroux B, Lindblad A, Richman J, Safford M, Ship J, Thompson VP, Williams OD, Yin W. Risk factors for osteonecrosis of the jaws: a case-control study from the CONDOR dental PBRN. J Dent Res. 2011; 90:439–44. [PubMed: 21317246]

37. Ali-Erdem M, Burak-Cankaya A, Cemil-Isler S, Demircan S, Soluk M, Kasapoglu C, Korhan-Oral C. Extraction socket healing in rats treated with bisphosphonate: animal model for bisphosphonate related osteonecrosis of jaws in multiple myeloma patients. Med Oral Patol Oral Cir Bucal. 2011; 16:e879–83. [PubMed: 21743422]

38. Dimopoulos MA, Kastritis E, Bamia C, Melakopoulos I, Gika D, Roussou M, Migkou M, Eleftherakis-Papaiakovou E, Christoulas D, Terpos E, Bamias A. Reduction of osteonecrosis of the jaw (ONJ) after implementation of preventive measures in patients with multiple myeloma treated with zoledronic acid. Ann Oncol. 2009; 20:117–20. [PubMed: 18689864]

39. Ripamonti CI, Maniezzo M, Campa T, Fagnoni E, Brunelli C, Saibene G, Bareggi C, Ascani L, Cislaghi E. Decreased occurrence of osteonecrosis of the jaw after implementation of dental preventive measures in solid tumour patients with bone metastases treated with bisphosphonates. The experience of the National Cancer Institute of Milan. Ann Oncol. 2009; 20:137–45. [PubMed: 18647964]

40. Graves DT, Kang J, Andriankaja O, Wada K, Rossa C Jr. Animal models to study host-bacteria interactions involved in periodontitis. Front Oral Biol. 2012; 15:117–32. [PubMed: 22142960]

41. Kalueff AV, Minasyan A, Keisala T, Shah ZH, Tuohimaa P. Hair barbering in mice: implications for neurobehavioural research. Behav Processes. 2006; 71:8–15. [PubMed: 16236465]

42. Sarna JR, Dyck RH, Whishaw IQ. The Dalila effect: C57BL6 mice barber whiskers by plucking. Behav Brain Res. 2000; 108:39–45. [PubMed: 10680755]

43. Long SY. Hair-nibbling and whisker-trimming as indicators of social hierarchy in mice. Anim Behav. 1972; 20:10–2. [PubMed: 4677163]

44. Russell RG, Rogers MJ. Bisphosphonates: from the laboratory to the clinic and back again. Bone. 1999; 25:97–106. [PubMed: 10423031]

45. Arce K, Assael LA, Weissman JL, Markiewicz MR. Imaging findings in bisphosphonate-related osteonecrosis of jaws. J Oral Maxillofac Surg. 2009; 67:75–84. [PubMed: 19371818]

46. Fedele S, Porter SR, D'Aiuto F, Aljohani S, Vescovi P, Manfredi M, Arduino PG, Broccoletti R, Musciotto A, Di Fede O, Lazarovici TS, Campisi G, Yarom N. Nonexposed variant of bisphosphonate-associated osteonecrosis of the jaw: a case series. Am J Med. 2010; 123:1060–4. [PubMed: 20851366]

47. Marx RE. Osteoradionecrosis: a new concept of its pathophysiology. J Oral Maxillofac Surg. 1983; 41:283–8. [PubMed: 6572704]

48. Ruggiero SL, Mehrotra B, Rosenberg TJ, Engroff SL. Osteonecrosis of the jaws associated with the use of bisphosphonates: a review of 63 cases. J Oral Maxillofac Surg. 2004; 62:527–34. [PubMed: 15122554]

49. Marx, R. Oral and intravenous bisphosphonate induced osteonecrosis of the jaws: history, etiology, prevention, and treatment. 2. 2007.

50. Devlin H, Horner K, Ledgerton D. A comparison of maxillary and mandibular bone mineral densities. J Prosthet Dent. 1998; 79:323–7. [PubMed: 9553887]

51. Kingsmill VJ, Gray CM, Moles DR, Boyde A. Cortical vascular canals in human mandible and other bones. J Dent Res. 2007; 86:368–72. [PubMed: 17384034]

Highlights

- Naturally occurring maxillary periradicular infections arise spontaneously in mice.
- We explored formation of ONJ-like lesions around such maxillary lesions.
- Animals were treated with RANKL inhibitors or with zoledronic acid.
- Same radiographic and histologic ONJ features were noted for all antiresorptives.
- This novel ONJ model using natural lesions bypasses experimental interventions.

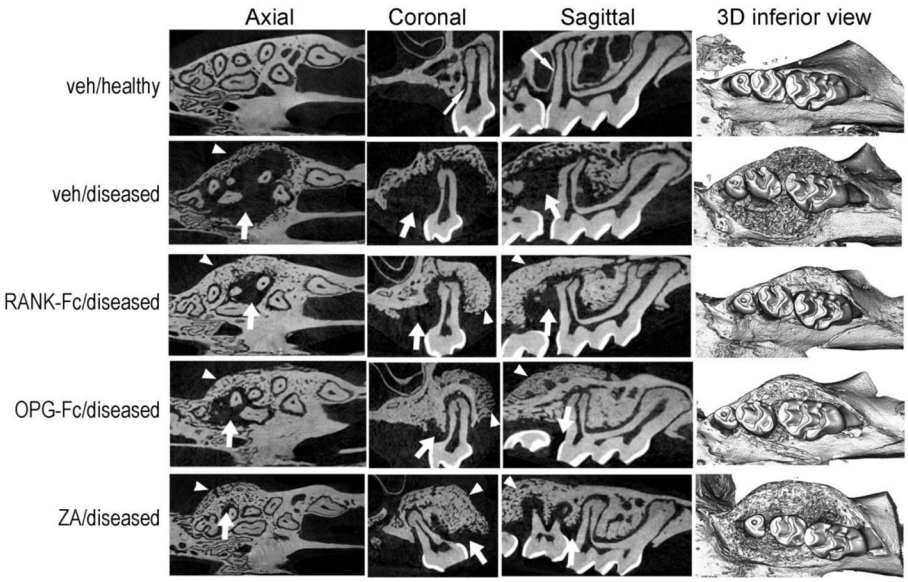

Figure 1.

Radiographic changes of the maxillary alveolar ridge. Representative axial, coronal and sagittal μCT slices and three-dimensional views of the maxillary molars of healthy (veh) or diseased site from veh, RANK-Fc, OPG-Fc and ZA treated animals are shown. Thin arrows point to the lamina dura around the roots of the veh/healthy animals. Thick arrows point to areas of osteolysis and arrowheads to areas or bone expansion in the diseased site of veh, RANK-Fc, OPG-Fc and ZA treated mice.

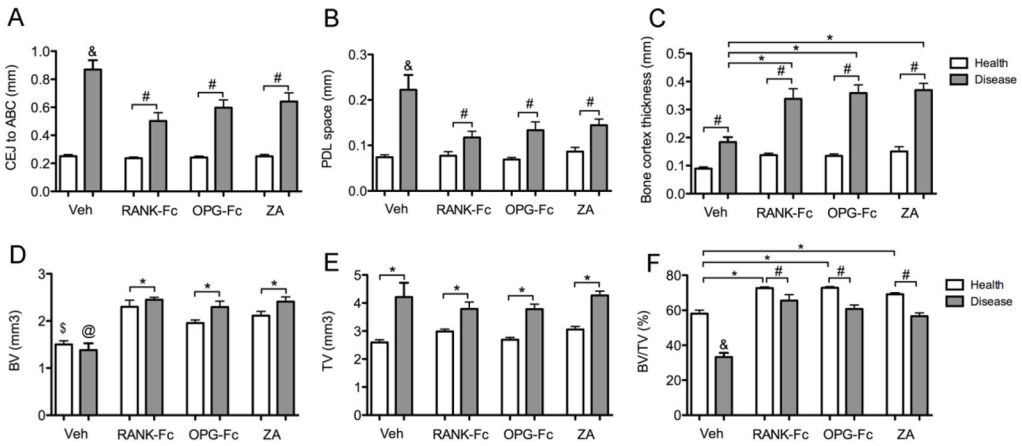

Figure 2.

Quantification of radiographic findings in the healthy and diseased sites of veh, RANK-Fc, OPG-Fc and ZA treated mice. To quantify amount of bone loss, the distance from the CEJ to the alveolar bone crest (ABC) was measured at the distal surface of the 1st molar (A) and the width of the PDL space was measured at the furcation area of the 1st molar (B). To assess alveolar bone expansion, the thickness of the buccal bone was measured, at the level of the apical third of the roots (C). To quantify the changes in the bone architecture, BV (D), TV (E) and BV/TV (F) was measured at the area of the alveolar ridge. &, statistically significantly different from healthy veh, diseased RANK-Fc, diseased OPG-Fc or diseased ZA, $p<0.001$. *, statistically significantly different from indicated groups, $p < 0.05$. #, statistically significantly different from indicated groups, $p < 0.01$. $, statistically different from healthy RANK-Fc, healthy OPG-Fc or healthy ZA, $p<0.01$. @, statistically significantly different from diseased RANK-Fc, diseased OPG-Fc or diseased ZA, $p<0.01$.

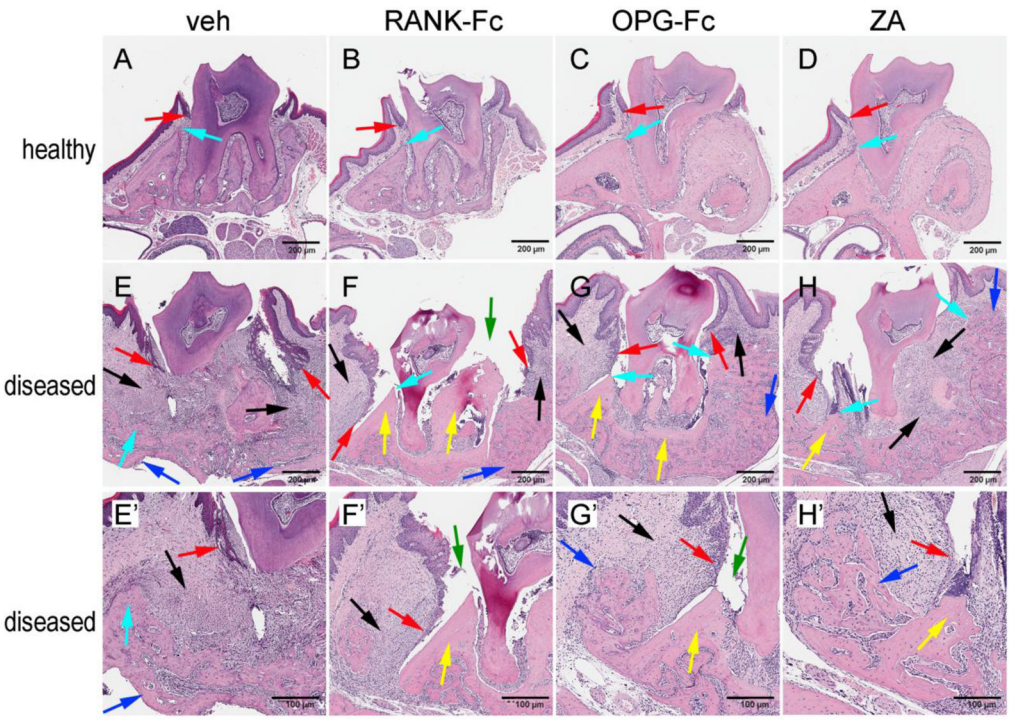

Figure 3.

Histologic examination of the periodontal and alveolar bone area. Healthy site of (A) veh, (B) RANK-Fc, (C) OPG-Fc, and (D) RANK-Fc treated animals. Diseases site of (E, E′) veh, (F, F′) RANK-Fc, (G, G′) OPG-Fc and (H, H′) ZA treated animals. Red arrows point to marginal gingival epithelium, turquoise arrows to alveolar crest, black arrows to areas of inflammation, blue arrows to periosteal bone deposition, yellow arrows to osteonecrotic areas, and green arrows to areas of bone exposure.

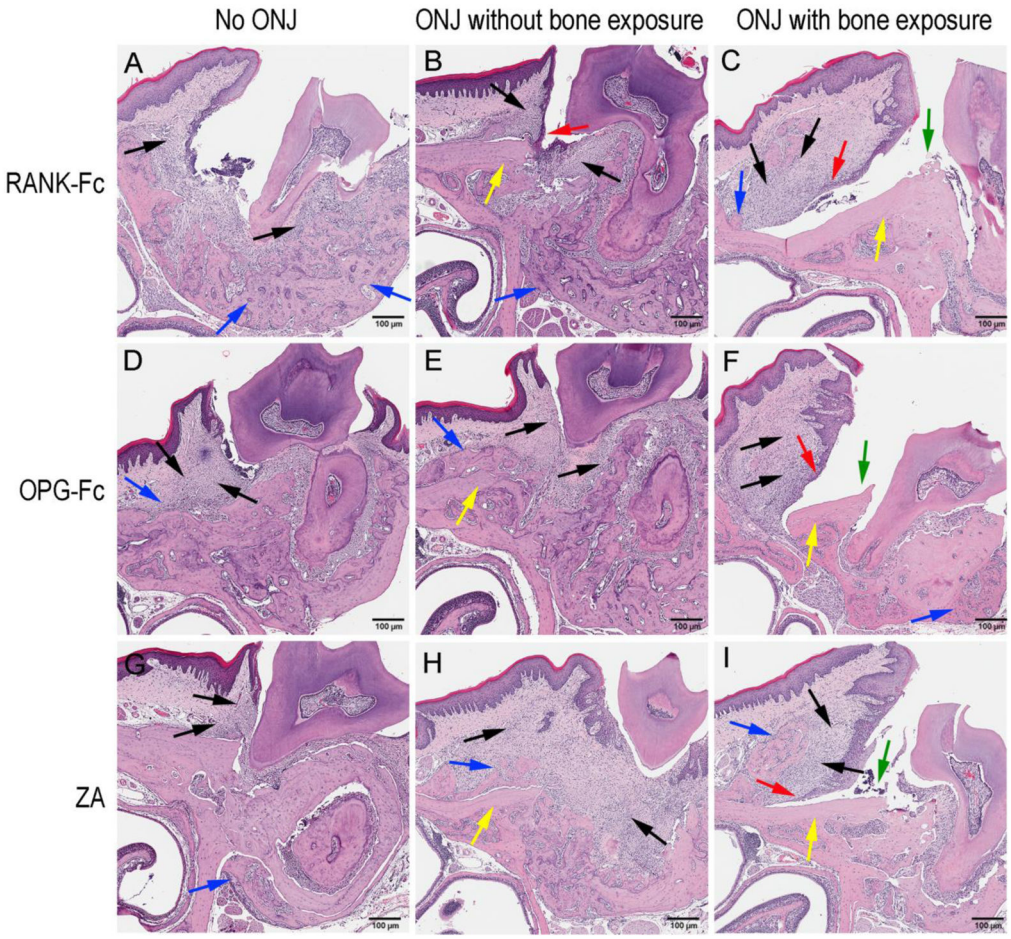

Figure 4.

Three histologic presentations of the diseased site in mice treated with antiresorptives. (A, B, and C) are RANK-Fc, (D, E, and F) are OPG-Fc and (G, H, and I) are ZA treated animals. (A, D, G) no osteonecrosis, (B, E, H) presence of osteonecrosis, (C, F, I) presence osteonecrosis with bone exposure were noted. Red arrows point to marginal gingival epithelium, black arrows to areas of inflammation, blue arrows to periosteal bone deposition, yellow arrows to osteonecrotic areas, and green arrows to areas of bone exposure.

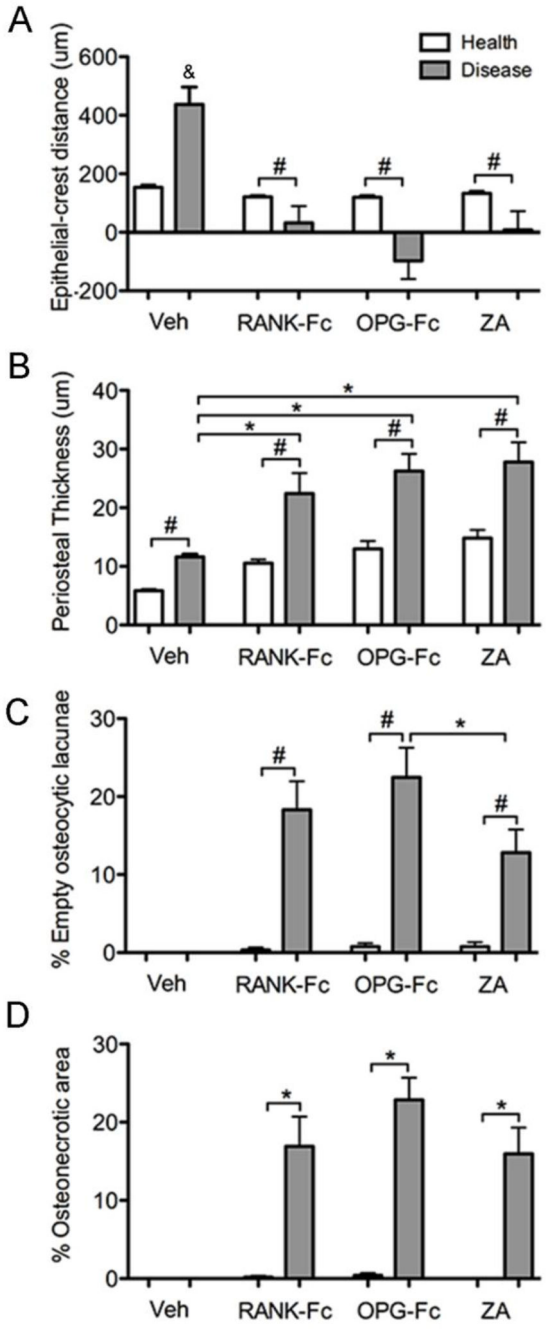

Figure 5.

Quantification of the histologic findings in the healthy and diseases sites of veh, RANK-Fc, OPG-Fc and ZA treated animals. (A) The shortest epithelial-crest distance was determined. If epithelium extended below the level of the alveolar crest, a negative value was assigned to the measurements. (B) Periosteal thickness, (C) % empty osteocytic lacunae and (D) % osteonecrotic area. &, statistically significantly different from healthy veh, diseased RANK-Fc, diseased OPG-Fc or diseased ZA, $p<0.001$. *, statistically significantly different from

indicated groups, $p < 0.05$. #, statistically significantly different from indicated groups, $p < 0.01$.

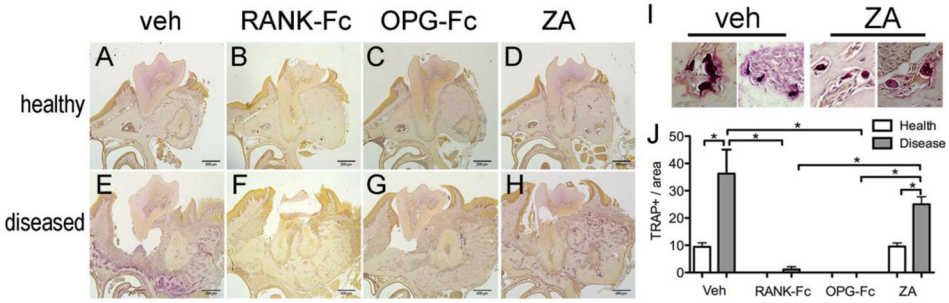

Figure 6.

RAP staining on histologic sections from healthy (A, B, C, and D) and diseased sites (E, F, G and H) from veh, RANK-Fc, OPG-Fc and ZA treated animals respectively. Select TRAP+ multinucleated cells from veh (I) and ZA (J) treated mice. Quantification TRAP+ cells in the veh, RANK-Fc, OPG-Fc and ZA treated animals (K). *Statistically significantly different, $p < 0.05$.

Table 1

Radiographic and histologic findings in veh and antiresorptive treatment groups

Group	Total hemimaxillae	Healthy (%)	Diseased (%)	Bone Expansion (%)	Osteonecrosis (%)	Bone Exposure (%)
Veh	33	20 (60.6)*	13 (39.4)*	13 (39.4)* (100)#	0** (0)* (0)#	0** (0)* (0)# (0)+
RANK- Fc	40	19 (47.5)*	21 (52.5)*	21 (52.5)* (100)#	10 (25)* (47)#	7 (17.5)* (33.3)# (70)+
OPG-Fc	40	19 (47.5)*	21 (52.5)*	21 (52.5)* (100)#	15 (37.5)* (71)#	11 (27.5)* (52)# (73)+
ZA	38	16 (42)*	22 (58)*	22 (58)* (100)#	10 (26.3)* (45)#	8 (21)* (36.4)# (80)+

** statistically significantly different compared to the RANK-Fc, OPG-Fc or ZA groups, $p<0.05$

* % of total hemimaxillae

% of diseased hemimaxillae

+ % of hemimaxillae with osteonecrosis